DEPARTMENT OF MATHEMATICS

Decomposition methods for wave scattering by topography with application to ripple beds

P. G. Chamberlain

and

D. Porter

Applied Mathematics Report 94/2

THE UNIVERSITY OF READING

Decomposition methods for wave scattering by topography with application to ripple beds

P. G. Chamberlain
and
D. Porter

Department of Mathematics, University of Reading
P. O. Box 220, Whiteknights
Reading, RG6 2AX.

August 19, 1994

Abstract

A method is described for determining those approximations to wave scattering by bed topography which are based on second-order ordinary differential equations. The development of a decomposition method allows the scattering matrix for an extended section of varying topography to be assembled in a piecemeal fashion. In particular, the scattering matrix for a ripple bed, consisting of an arbitrary number of periodic undulations, is expressed in terms of the scattering properties of a single ripple. The structure obtained reveals the main features of ripple bed scattering, including resonant reflection at certain frequencies. The analysis is allied to numerical calculations to compare five different models of ripple bed scattering.

1 Introduction

A number of approximations have recently been devised to the scattering of water waves by a ripple bed, which consists of a section of periodic undulations set in an otherwise flat, horizontal bed. The presence of resonant peaks in the amplitude of the wave reflected by a ripple bed has attracted particular attention and the ability of a model of wave scattering by topography to predict these peaks has been used as a measure of its validity.

The investigation described in this paper was provoked by one particular feature of approximations to scattering by ripple bed, noticed in numerical computations. It was found that different models of the scattering process can give quite different scattered wave fields for a single ripple, but very similar fields for a sufficiently large number of ripples. This phenomenon applies, for example, to the modified mild-slope equation of Chamberlain and Porter [5] and Kirby's [7] extended mild-slope equation. On the other hand, the mild-slope equation of Berkhoff [1], [2] produces different results again for one ripple and does not always give acceptable results for several ripples.

The initial aim was to identify the process which can, in some cases, erase the discrepancies in the scattered wave amplitude predicted by different models, as the number of ripples increases.

We are concerned only with a particular class of such models in which scattering by two-dimensional topography is approximated by a second-order ordinary differential equation. Such an equation arises by the removal of the vertical coordinate from the full linear boundary value problem for scattering. Chamberlain and Porter [5] have recently given an account of this approximation method. To encompass the three models equations referred to above, and variants of them, we base the development on a general second-order ordinary differential equation, specifying only minimal requirements on its coefficients.

The investigation has two main strands. We first show that the amplitudes of the scattered waves for any given bed topography are given in terms of the boundary values of any two linearly independent solutions of the underlying differential equation. Ultimately we choose to generate two solutions by solving initial value problems, thus reducing the numerical calculations to the simplest possible form. The inherent structure of the problem is thereby detached from the numerical solution process, as far as this is possible. In this sense, the present method contrasts with Chamberlain's [3] approach to the mild-slope equation.

The objective in consigning the computational aspects of the problem to a subsidiary role is that it allows certain properties of the solution to be identified analytically. We can show, for instance, that certain relationships between the scattered wave amplitudes, established by Newman [9] for the full linear wave scattering problem, also hold for all approximations to that problem, of the type considered here. These so-called symmetry relationships are an intrinsic part of the problem rather than of its exact solution, in the sense that they are automatically satisfied, whatever the accuracy of the solution. Thus, for example, the fact that the wave energy balance equation is satisfied does not imply that an accurate solution has been determined. This information allows the relationships to be used, even for approximate solutions, as well as disqualifying them as checks on numerical solutions. In fact, a further relationship, not found by Newman, can be retained as a check, if used correctly, as we describe in Section 2.

The second main part of the development exploits and extends the decomposition method, introduced by Chamberlain [4]. This method consists of assembling the scattering properties of an extended topography from those of its constituent parts. Topography can thus be decomposed into a number of convenient elements and the scattering characteristics of each element determined independently of the others.

This approach is particularly significant in relation to ripple beds. By using decomposition and the symmetry relationships referred to earlier, we derive explicit formulae for the scattered wave amplitudes for a patch consisting of an arbitrary number of ripples in terms of those for a single ripple. Numerical calculations are therefore required for only one ripple. In addition to the obvious computational saving, the replication formulae which generate the wave field for several ripples from that for one ripple meet our initial objective. The mechanism which produces the resonant peaks referred to earlier is apparent in the structure of the replication formulae.

The paper is organised in the following way. In Section 2 we develop an efficient solution method and deduce the intrinsic symmetry relationships, for any bed topography. Section 3 develops the decomposition process which leads to the ripple bed replication formulae. The remaining two sections are devoted to the implementation of the methods. In Section 4 we select, and briefly describe, a particular numerical method and list five equations of the type under consideration. These equations provide the basis for the results given in the final section, where we illustrate and discuss the established theoretical features of scattering by ripple beds.

2 The scattering matrix

We consider approximations to wave scattering on water in which the free surface elevation is given by $\mathrm{Re}(\eta(x)e^{-i\sigma t})$ where the angular frequency σ is assigned and η satisfies the equation

$$\eta''(x) + p\eta'(x) + q\eta(x) = 0 \qquad (-\infty < x < \infty). \tag{2.1}$$

Here $p(x)$ and $q(x)$ are given real-valued functions which depend on the still water depth $h(x)$ and are such that

(i) $p = 0$ and $q = k^2$ where h is a constant, k being a constant depending on h;

(ii) $\int_{x_0}^{x_1} p(x)\mathrm{d}x = 0$ for any points x_0 and x_1 such that $h(x_0) = h(x_1)$.

We assume that p, q and h are continuous and require η and η' to be continuous.

One further stipulation is made, that

$$h(x) = \begin{cases} h_m & (x \le l_m), \\ h_n & (x \ge l_n > l_m), \end{cases}$$

where h_m and h_n are constants. Throughout this account, m and n denote natural numbers with $m < n$. The subscript notation is introduced in anticipation of the decomposition method described later.

It follows from our assumptions that

$$\eta(x) = \left\{ \begin{array}{ll} A_{m,n}e^{ik_m(x-l_m)} + B_{m,n}e^{ik_m(l_m-x)} & (x \le l_m), \\ A_{n,m}e^{ik_n(l_n-x)} + B_{n,m}e^{ik_n(x-l_n)} & (x \ge l_n), \end{array} \right\} \tag{2.2}$$

where the constant wavenumbers k_m and k_n are those corresponding to the depths h_m and h_n, respectively. The prescribed amplitudes $A_{m,n}$ and $A_{n,m}$ of the incoming waves and the amplitudes $B_{m,n}$ and $B_{n,m}$ of the scattered waves, which are to be determined, are related by a scattering matrix $S_{m,n}$ defined by

$$\begin{pmatrix} B_{m,n} \\ B_{n,m} \end{pmatrix} = S_{m,n} \begin{pmatrix} A_{m,n} \\ A_{n,m} \end{pmatrix}, \qquad S_{m,n} = \begin{pmatrix} R_{m,n} & T_{n,m} \\ T_{m,n} & R_{n,m} \end{pmatrix}. \tag{2.3}$$

The scattering coefficients $R_{m,n}$ ($R_{n,m}$) and $T_{m,n}$ ($T_{n,m}$) are, to within known phase terms, the amplitudes of the reflected and transmitted waves respectively, corresponding to a wave of unit amplitude from the left (right). Our principle aim is to determine $S_{m,n}$.

The core of the problem is to solve

$$\eta''(x) + p\eta'(x) + q\eta(x) = 0 \qquad (l_m < x < l_n) \tag{2.4}$$

subject to continuity of η and η' at $x = l_m, l_n$. This continuity, used in conjunction with (2.2), provides boundary conditions for (2.4) in the form

$$\eta'(l_m) + ik_m\eta(l_m) = 2ik_mA_{m,n}, \qquad \eta'(l_n) - ik_n\eta(l_n) = -2ik_nA_{n,m} \tag{2.5}$$

and shows that the scattered wave amplitudes can be found from

$$B_{m,n} = \eta(l_m) - A_{m,n}, \qquad B_{n,m} = \eta(l_n) - A_{n,m}. \tag{2.6}$$

Now let η_1 and η_2 denote real-valued, linearly independent solutions of (2.4) and note that their Wronskian

$$w(x) = \eta_1(x)\eta_2'(x) - \eta_2(x)\eta_1'(x) = w_0 \exp\left(-\int_{l_m}^{x} p(\xi)\mathrm{d}\xi\right), \tag{2.7}$$

where w_0 is a real, non-zero constant. The function $\eta = a_1\eta_1 + a_2\eta_2$ satisfies (2.4) and it also satisfies (2.5) if the constants a_1 and a_2 can be chosen so that

$$a_1f^+_{m,1} + a_2f^+_{m,2} = 2ik_mA_{m,n}, \qquad a_1f^-_{n,1} + a_2f^-_{n,2} = -2ik_nA_{n,m}$$

where

$$f^{\pm}_{\alpha,j} = \eta_j'(l_\alpha) \pm ik_\alpha\eta_j(l_\alpha) \qquad (\alpha = m, n, \quad j = 1, 2). \tag{2.8}$$

If we introduce the matrices

$$F = \begin{pmatrix} f^+_{m,1} & f^+_{m,2} \\ f^-_{n,1} & f^-_{n,2} \end{pmatrix}, \quad D = \begin{pmatrix} k_m & 0 \\ 0 & -k_n \end{pmatrix}, \quad \Psi = \begin{pmatrix} \eta_1(l_m) & \eta_2(l_m) \\ \eta_1(l_n) & \eta_2(l_n) \end{pmatrix}, \tag{2.9}$$

which are related by $F - \overline{F} = 2iD\Psi$, we see that a_1 and a_2 satisfy

$$F\begin{pmatrix} a_1 \\ a_2 \end{pmatrix} = 2iD\begin{pmatrix} A_{m,n} \\ A_{n,m} \end{pmatrix}$$

and that (2.6) implies

$$\begin{pmatrix} B_{m,n} \\ B_{n,m} \end{pmatrix} = \Psi\begin{pmatrix} a_1 \\ a_2 \end{pmatrix} - \begin{pmatrix} A_{m,n} \\ A_{n,m} \end{pmatrix}.$$

Assuming for the moment that F is non-singular, we can eliminate $(a_1, a_2)^T$ between the last two equations to give

$$\begin{pmatrix} B_{m,n} \\ B_{n,m} \end{pmatrix} = -D^{-1}\overline{F}F^{-1}D\begin{pmatrix} A_{m,n} \\ A_{n,m} \end{pmatrix}.$$

Reference to (2.3) shows that

$$S_{m,n} = -D^{-1}\overline{F}F^{-1}D, \tag{2.10}$$

which determines the scattering coefficients in terms of the wavenumbers k_m and k_n and the boundary values of η_1 and η_2 and their derivatives. The problem is therefore solved by calculating the boundary values of any two linearly independent solutions of (2.4).

There remains the issue of whether F is invertible. Suppose that there exists a particular pair of linearly independent solutions η_1 and η_2 for which F is non-singular and consider a different such pair, say $\hat{\eta}_1$ and $\hat{\eta}_2$, with the corresponding matrix F written as $\hat{F}$. Clearly, there exist constants a, b, c and d such that $\hat{\eta}_1 = a\eta_1 + b\eta_2$ and $\hat{\eta}_2 = c\eta_1 + d\eta_2$ with $ad - bc \neq 0$ and it is easy to verify that $\det(\hat{F}) = (ad - bc)\det(F)$. It is shown in Section 4 that there is a particular linearly independent pair of solutions of (2.4) for which F^{-1} exists and hence F is non-singular for every linearly independent pair.

Certain relationships between the scattering coefficients follow directly from (2.10) which implies that $S_{m,n}\overline{S}_{m,n} = \overline{S}_{m,n}S_{m,n} = I$ and that consequently $|\det(S_{m,n})| = 1$. Therefore

$$|R_{m,n}|^2 + \overline{T}_{m,n}T_{n,m} = |R_{n,m}|^2 + T_{m,n}\overline{T}_{n,m} = 1,$$

$$R_{n,m}\overline{T}_{m,n} + \overline{R}_{n,m}T_{m,n} = \overline{R}_{n,m}T_{n,m} + R_{m,n}\overline{T}_{n,m} = 0,$$

$$|R_{m,n}R_{n,m} - T_{m,n}T_{n,m}| = 1,$$

from which follow the further identities

$$\left.\begin{aligned} |R_{n,m}R_{m,n}| + |T_{m,n}T_{n,m}| &= 1, \\ |R_{n,m}| &= |R_{m,n}|, \\ \arg(T_{m,n}) - \arg(T_{n,m}) &= 2\alpha_1\pi, \\ \arg(R_{m,n}R_{n,m}) - \arg(T_{m,n}T_{n,m}) &= (2\alpha_2 + 1)\pi, \end{aligned}\right\} \tag{2.11}$$

for some integers α_1 and α_2.

Explicit expressions for the components of $S_{m,n}$ are given by (2.9) and (2.10) in the form

$$S_{m,n} = Q_{m,n}^{-1}\begin{pmatrix} -P_{m,n} & 2ik_n w_m \\ 2ik_m w_n & -\overline{P}_{m,n} \end{pmatrix}, \tag{2.12}$$

where (2.7) and (2.8) have been used to simplify the off-diagonal terms,

$$P_{m,n} = \overline{f}_{m,1}^{+}f_{n,2}^{-} - \overline{f}_{m,2}^{+}f_{n,1}^{-}, \qquad Q_{m,n} = f_{m,1}^{+}f_{n,2}^{-} - f_{m,2}^{+}f_{n,1}^{-}, \tag{2.13}$$

and $w_\alpha = w(l_\alpha)$ for $\alpha = m, n$. We note that $|P_{m,n}|^2 + 4k_m k_n w_m w_n = |Q_{m,n}|^2$ is a consequence of $|\det(\overline{F}F^{-1})| = 1$ and that the identity

$$k_m w_n |T_{n,m}| = k_n w_m |T_{m,n}| \tag{2.14}$$

follows from (2.3) and (2.12).

Chamberlain [4] has established the identities (2.11) and particular forms of (2.14) for the mild-slope equation and extended mild-slope equation (which are given in Section 4). Here we have shown that the identities hold for any approximation to scattering by bed topography governed by an equation of the form (2.1). We have shown, moreover, that the identities (2.11) are satisfied not only by the components of the exact scattering matrix $S_{m,n}$ but also by any approximation to these components. Thus if we assign arbitrary values to $\eta_j(l_\alpha)$, $\eta_j'(l_\alpha)$, for $\alpha = m, n$ and $j = 1, 2$, the components of $S_{m,n}$ evaluated from (2.12) will necessarily satisfy (2.11). The same remarks apply to (2.14), if the chosen boundary values of η_1 and η_2 are consistent with (2.7). However, if the values w_m and w_n of the Wronskian are calculated approximately as part of the process of solving (2.4) for η_1 and η_2, (2.14) will not generally be satisfied. Used in this sense, (2.14) is the only relationship of its type which can serve as a check on the accuracy of a numerical solution.

3 Decomposition, recurrence relations and replication formulae

Suppose now that the undulating section of the bed occupies the interval (l_1, l_N). By decomposing the undulations into $N-1$ sections occupying the contiguous intervals (l_m, l_{m+1}) for $m = 1, 2, \ldots, N-1$, the overall scattering matrix $S_{1,N}$ can be constructed from the scattering matrices for the individual sections.

The notation has been devised with decomposition in mind and we need to note only that the incoming and outgoing waves to the left of (l_1, l_2) and to the right of (l_{N-1}, l_N) are also those for the whole interval (l_1, l_N). Thus, referring to (2.2), we have

$$A_{1,2} = A_{1,N}, \quad B_{1,2} = B_{1,N}, \quad A_{N,N-1} = A_{N,1}, \quad B_{N,N-1} = B_{N,1}. \tag{3.1}$$

According to (2.3), the scattering properties of the individual sections are given by

$$\begin{pmatrix} B_{m,m+1} \\ B_{m+1,m} \end{pmatrix} = S_{m,m+1} \begin{pmatrix} A_{m,m+1} \\ A_{m+1,m} \end{pmatrix} \qquad (m = 1, 2, \ldots, N-1) \tag{3.2}$$

and these are supplemented by the matching conditions

$$B_{m,m-1} = A_{m,m+1}, \quad A_{m,m-1} = B_{m,m+1} \qquad (m = 2, 3, \ldots, N-1), \tag{3.3}$$

which ensure that the wave amplitudes coincide at the interfaces between adjacent sections. The coupled (tridiagonal) system consisting of (3.2) and (3.3) can be solved for $B_{1,2}$ and $B_{N,N-1}$ in terms of $A_{1,2}$ and $A_{N,N-1}$ and this allows $S_{1,N}$ to be constructed using (2.3) and (3.1).

A recurrence formula for solving the system can be derived directly by decomposing the interval (l_1, l_{n+1}) into (l_1, l_n) and (l_n, l_{n+1}). From (2.3) we have

$$\begin{pmatrix} B_{1,n} \\ B_{n,1} \end{pmatrix} = S_{1,n} \begin{pmatrix} A_{1,n} \\ A_{n,1} \end{pmatrix}, \qquad \begin{pmatrix} B_{n,n+1} \\ B_{n+1,n} \end{pmatrix} = S_{n,n+1} \begin{pmatrix} A_{n,n+1} \\ A_{n+1,n} \end{pmatrix},$$

and the corresponding matching conditions are $A_{n,1} = B_{n,n+1}$ and $B_{n,1} = A_{n,n+1}$. Solving for $B_{1,n}$ and $B_{n+1,n}$ in terms of $A_{1,n}$ and $A_{n+1,n}$ and using the adopted convention for labelling the scattering coefficients, it is readily found that

$$S_{1,n+1} = \frac{1}{1 - R_{n,1}R_{n,n+1}} \begin{pmatrix} R_{1,n} - R_{n,n+1}\det(S_{1,n}) & T_{n,1}T_{n+1,n} \\ T_{1,n}T_{n,n+1} & R_{n+1,n} - R_{n,1}\det(S_{n,n+1}) \end{pmatrix}, \tag{3.4}$$

which holds for $n = 2, 3, \ldots, N-1$. Thus $S_{1,n}$ can be determined successively for $n = 3, 4, \ldots, N$ once $S_{n,n+1}$ is known for $n = 1, 2, \ldots, N-1$. This process, which is equivalent to solving (3.2) and (3.3), is valid provided that $R_{n,1}R_{n,n+1} \neq 1$ for $n = 2, 3, \ldots, N-1$. It is not difficult to show that, if $R_{m,1}R_{m,m+1} = 1$ for some m satisfying $2 \leq m \leq N-1$, then (3.4) is replaced by $S_{1,n+1} = \mathrm{diag}(R_{1,n}, R_{n+1,n})$ for $n = m-1, m, \ldots, N-1$. Thus the section (l_1, l_n) is purely reflecting for $n = m, m+1, \ldots, N$.

Further progress can be made if the bed undulations are periodic, for then the recurrence relations implied by (3.4) can be solved explicitly. Suppose, then, that there is an identical bed shape on each of the intervals (l_m, l_{m+1}) for $m = 1, 2, \ldots, N-1$. Obviously $S_{n,n+1} = S_{1,2}$ for $n = 1, 2, \ldots, N-1$, allowing us to deduce from (3.4) that

$$\left.\begin{aligned} R_{1,n+1} &= R_{1,n} + \Delta_n^{-1}T_{1,n}T_{n,1}R_{1,2}, && \text{(a)} \\ T_{1,n+1} &= \Delta_n^{-1}T_{1,n}T_{1,2}, && \text{(b)} \\ R_{n+1,1} &= R_{2,1} + \Delta_n^{-1}T_{1,2}T_{2,1}R_{n,1}, && \text{(c)} \\ T_{n+1,1} &= \Delta_n^{-1}T_{n,1}T_{2,1}, && \text{(d)} \end{aligned}\right\} \quad (n = 1, 2, \ldots, N-1), \tag{3.5}$$

where

$$\Delta_n = 1 - R_{n,1}R_{1,2}. \tag{3.6}$$

We can solve (3.5) for the components of $S_{1,N}$ in terms of those of $S_{1,2}$ on the assumption that $T_{1,2} \neq 0$. (If $T_{1,2} = 0$, the situation is trivial and $R_{N,1} = R_{2,1}$, $R_{1,N} = R_{1,2}$ and $T_{1,N} = T_{N,1} = 0$.) We also assume that $T_{1,2} = T_{2,1}$, although this is not necessary for the solution of (3.5) to proceed. It is, however, a consequence of (2.11) and (2.14) in the present circumstances since $h(l_1) = h(l_2)$ implies that $k_1 = k_2$ and $w_1 = w_2$ (because $\int_{l_1}^{l_2} p(\xi)\mathrm{d}\xi = 0$).

It is shown in the Appendix that

$$\left.\begin{aligned} R_{1,N} &= R_{1,2}\sigma_N(\sigma_N - T_{2,1}\sigma_{N-1})^{-1}, \\ R_{1,2}R_{N,1} &= R_{2,1}R_{1,N}, \\ T_{1,N} &= T_{1,2}(\sigma_N - T_{2,1}\sigma_{N-1})^{-1}, \\ T_{N,1} &= T_{1,N}, \end{aligned}\right\} \tag{3.7}$$

where the real numbers σ_N and σ_{N-1} are determined by the recursion relation

$$\left.\begin{aligned} &\sigma_{n+1} - 2\frac{\cos(\arg(T_{1,2}))}{|T_{1,2}|}\sigma_n + \sigma_{n-1} = 0 \qquad (n = 2, 3, \ldots, N-1), \\ &\sigma_1 = 0, \quad \sigma_2 = 1. \end{aligned}\right\} \tag{3.8}$$

It is also deduced in the Appendix that

$$\left.\begin{aligned} |R_{1,N}|^2 &= |R_{1,2}|^2\sigma_N^2\left(|R_{1,2}|^2\sigma_N^2 + |T_{1,2}|^2\right)^{-1}, \\ |R_{1,2}||R_{N,1}| &= |R_{2,1}||R_{1,N}|, \\ |T_{1,N}| &= |T_{1,2}|\left(|R_{1,2}|^2\sigma_N^2 + |T_{1,2}|^2\right)^{-1}, \\ |T_{N,1}| &= |T_{1,N}|. \end{aligned}\right\} \tag{3.9}$$

These formulae reduce the computation of the scattering matrix for an arbitrary number of ripples to that for a single ripple. They also reveal some aspects of the process of scattering by ripple beds as we indicate in Section 5.

4 Implementation

The general scattering problem posed has been reduced to that of finding any two real-valued, linearly independent functions η_1 and η_2 satisfying

$$\eta_j''(x) + p\eta_j'(x) + q\eta_j(x) = 0 \qquad (l_m < x < l_n, \quad j = 1, 2), \tag{4.1}$$

possibly for a number of intervals (l_m, l_n). More precisely, we require only the boundary values $\eta_j(l_\alpha)$, $\eta_j'(l_\alpha)$ for $j = 1, 2$ and $\alpha = m, n$ to construct

the scattering matrix $S_{m,n}$ using (2.12). As two boundary values may be specified for each function, four boundary values in all are to be determined.

We could follow Chamberlain [3] by using variational principles in conjunction with integral equations to estimate the required values. Indeed, the freedom we have to choose four boundary values can be exercised to produce simpler integral equations than those encountered by Chamberlain.

However, we adopt a different strategy by imposing initial conditions on η_1 and η_2, namely

$$\eta_1(l_m) = \eta_2'(l_m) = 1, \qquad \eta_1'(l_m) = \eta_2(l_m) = 0, \tag{4.2}$$

which implies that the Wronskian (2.7) is given by

$$w(x) = \exp\left(-\int_{l_m}^{x} p(\xi)\mathrm{d}\xi\right). \tag{4.3}$$

Using the initial conditions (4.2) and referring to (2.9), it is not difficult to show that $\det(F) = 0$ implies that $w(l_n) \leq 0$, which contradicts equation (4.3). Hence F is invertible for the current choice of η_1 and η_2 (and hence for any other linearly independent pair η_1 and η_2 by the argument in Section 2).

The boundary values to be calculated are $\eta_j(l_n)$ and $\eta_j'(l_n)$ for $j = 1, 2$, in terms of which the quantities defined in (2.13) are given by

$$\left.\begin{aligned} P_{m,n} &= -ik_m(\eta_2'(l_n) - ik_n\eta_2(l_n)) - (\eta_1'(l_n) - ik_n\eta_1(l_n)), \\ Q_{m,n} &= ik_m(\eta_2'(l_n) - ik_n\eta_2(l_n)) - (\eta_1'(l_n) - ik_n\eta_1(l_n)). \end{aligned}\right\} \tag{4.4}$$

These, together with $w_m = w(l_m) = 1$ and $w_n = w(l_n)$ form the scattering matrix (2.12).

By choosing the initial conditions (4.2) the approximation process is greatly simplified, for we can call upon a large class of well-established numerical methods. We rewrite (4.1) as a coupled pair of first-order differential equations by introducing the function $\psi = \eta'$. Our aim therefore is to solve

$$\mathbf{y}' = \mathbf{f}(x, \mathbf{y})$$

in which $\mathbf{y} = (\eta, \psi)^T$ and $\mathbf{f} = (\psi, -p\psi - q\eta)^T$ where $\mathbf{y}(l_m)$ is given. The scattering matrix $S_{m,n}$ is known once $\mathbf{y}(l_n)$ is found and consequently a simple linear scheme of the form

$$\sum_{j=0}^{M} \alpha_j \mathbf{y}_{i+j} = \Delta x \sum_{j=0}^{M} \beta_j \mathbf{f}_{i+j} \qquad (i = 0, 1, \ldots, J - M),$$

in which $\Delta x = (l_n - l_m)/J$, $\mathbf{y}_j \approx \mathbf{y}(l_m + j\Delta x)$ and $\mathbf{f}_j = \mathbf{f}(l_m + j\Delta x, \mathbf{y}_j)$, is used to approximate $\mathbf{y}(l_n)$. Such numerical schemes are defined on choosing Δx,

M, α_j and β_j $(j = 0, 1, \ldots, M)$ and their use is well-documented (see Lambert [8] for example). For the purposes of results presented in this paper we use an implicit 3-step method (i.e. $M = 3$) which is accurate to $O(\Delta x)^4$. The two additional starting values required are approximated using the classical 4-stage 4th order Runge Kutta method.

The number of subintervals J in the interval (l_m, l_n) used in the linear scheme may be monitored using equation (2.14). As mentioned in Section 2 this relation is not automatically satisfied by approximate solutions to the problem. For ripple bed problems of the type discussed in Section 5 this check is most efficiently carried out over the extent of a complete ripple since in this case (2.14) reduces to $|T_{m,n}| = |T_{n,m}|$.

It only remains to give the different versions of equation (2.1) that we shall use to present results in the next section. These are as follows.

- The mild-slope equation.

$$(u_0\eta')' + k^2 u_0 \eta = 0. \tag{4.5}$$

- The modified mild-slope equation.

$$(u_0\eta')' + (k^2 u_0 + u_1 h' + u_2 h'')\eta = 0. \tag{4.6}$$

- An approximate mild-slope equation.

$$(\{u_0 - \delta(2u_1 + \operatorname{sech}^2 kh)\}\eta')' + k^2(u_0 - 2\delta u_1)\eta = 0. \tag{4.7}$$

- An approximate modified mild-slope equation.

$$(\{u_0 - \delta(2u_1 + \operatorname{sech}^2 kh)\}\eta')' + \left(k^2(u_0 - 2\delta u_1) - u_1\delta''\right)\eta = 0. \tag{4.8}$$

- Kirby's extended mild-slope equation.

$$(u_0\eta')' - \operatorname{sech}^2 kh(\delta\eta')' + k^2 u_0 \eta = 0. \tag{4.9}$$

The functions u_0, u_1 and u_2 are given by

$$\begin{aligned}
u_0 &= \frac{1}{2k}\tanh kh\left(1 + \frac{K}{\sinh K}\right), \\
u_1 &= \frac{\operatorname{sech}^2 kh}{4(K + \sinh K)}\{\sinh K - K\cosh K\}, \\
u_2 &= \frac{k\operatorname{sech}^2 kh}{12(K + \sinh K)^3}\Big\{K^4 + 4K^3\sinh K - 9\sinh K\sinh 2K \\
&\quad + 3K(K + 2\sinh K)(\cosh^2 K - 2\cosh K + 3)\Big\},
\end{aligned}$$

in which $K = 2kh$.

Note that in (4.5) and (4.6) h is the undisturbed fluid depth, whereas in (4.7), (4.8) and (4.9) the undisturbed depth is $h - \delta$ where h represents a slowly varying component of the depth onto which a small-amplitude, rapidly-varying component δ is superimposed.

In each of the five equations listed above the wavenumber k is the positive real root of the dispersion relation

$$\sigma^2 = gk \tanh(kh)$$

in which g is the acceleration due to gravity. Note that this definition of k implies that in equations (4.7), (4.8) and (4.9) k is independent of δ.

A derivation and discussion of these five equations may be found in Chamberlain and Porter [5].

5 Scattering by ripple beds

To illustrate the methods described above, numerically and analytically, we show how the principal features of scattering by ripple beds follow from the replication formulae.

These formula require the computation of the scattering matrix $S_{1,2}$ for a single cycle of the ripple formulation, located on (l_1, l_2). This is carried out as indicated in Section 4. We may then use (3.7), (3.8) and (3.9) to determine the scattering properties of N ripples.

We concentrate on the reflected wave amplitude $|R_{1,N}|$, to align with previous work, noting that $|R_{1,N}| = |R_{N,1}|$ and $|T_{1,N}| = |T_{N,1}| = \sqrt{1 - |R_{1,N}|^2}$ in the cases under consideration. The formulae

$$|R_{1,N}|^2 = |R_{1,2}|^2 \sigma_N^2 \left(|R_{1,2}|^2 \sigma_N^2 + |T_{1,2}|^2 \right)^{-1}, \qquad |R_{1,2}|^2 + |T_{1,2}|^2 = 1, \quad (5.1)$$

together with (3.8), therefore form the focus of attention.

If we introduce the quantities $\gamma \in \mathbb{R}$ and $\theta \in \mathbb{C}$ by

$$\gamma = \frac{\cos(\arg(T_{1,2}))}{|T_{1,2}|}, \qquad \cos(\theta) = \gamma, \quad (5.2)$$

it follows from (3.8) that

$$\sigma_n = \operatorname{cosec}(\theta) \sin((n-1)\theta) \qquad (n = 1, 2, \ldots, N). \quad (5.3)$$

The value of θ may be chosen as follows. If $|\gamma| \leq 1$, we take $0 \leq \theta \leq \pi$, interpreting (5.3) as $\sigma_n = (\pm 1)^n (n-1)$ if $\gamma = \pm 1$. If $\gamma > 1$, $\theta = i\omega$ (so

that $\sigma_n = \text{cosech}(\omega)\sinh((n-1)\omega))$ and if $\gamma < -1$, $\theta = \pi + i\omega$ (so that $\sigma_n = (-1)^n\text{cosech}(\omega)\sinh((n-1)\omega)$ with $\omega > 0$ in both cases.

This is a convenient point to remark that the formulae (3.7), with σ_n given by (5.3), can be deduced using Floquet theory. The quantity $i\theta/\mu$ is the characteristic exponent, in the sense of the account given by Ince [6], where $\mu = l_2 - l_1$ is the period of the ripple bed. Some care is needed to include the three cases for θ indicated above when using this alternative approach, which offers no advantages over the decomposition method.

Clearly $|R_{1,N}|$ depends on $|R_{1,2}|$ and γ, both of which may be considered to have been determined numerically. We envisage $|R_{1,2}|$ and γ as varying continuously with some parameter ($2k/\ell$ in the examples given later) and deduce the following properties of $|R_{1,N}|$, considered as a function of the same parameter.

(a) $|R_{1,N}| = 0$ where $|R_{1,2}| = 0$, for $N \geq 3$.

(b) $|R_{1,N}| = 0$, for each $N \geq 3$, where $\sigma_N = 0$. It follows easily from (5.3) that $|R_{1,N}| = 0$ where

$$\gamma = \cos(\alpha\pi/(N-1)) \qquad (\alpha = 1, 2, \ldots, N-2). \tag{5.4}$$

(c) Where $|\gamma| \geq 1$, $|\sigma_N|$ increases with N and $|\sigma_N| \to \infty$ as $N \to \infty$. Therefore, where $|\gamma| \geq 1$, the value of $|R_{1,N}|$ increases with N and $|R_{1,N}| \to 1$ as $N \to \infty$. The increase is more rapid, and the limit more rapidly approached, the larger $|\gamma|$.

(d) Where $|\gamma| < 1$, σ_N oscillates, perhaps rapidly, as N increases; $|\sigma_N|$ is bounded above by $|\text{cosec}(\theta)|$.

We infer from these remarks that the observed resonances in $|R_{1,N}|$ arise where $|\gamma| \geq 1$, irrespective of the value of $|R_{1,2}|$ there. Of course, where $|R_{1,2}|$ is small the resonant peaks will grow more slowly with N, by virtue of (5.1). We note that $|R_{1,2}| = 0$ implies that $|T_{1,2}| = 1$ and hence that $|\gamma| \leq 1$. Therefore, a prospective resonant peak of $|R_{1,N}|$ (for which $|\gamma| > 1$) cannot be annihilated by $|R_{1,2}| = 0$.

These properties can be illustrated by reference to specific examples of ripple beds and different model equations. We suppose that the ripple bed occupies the interval $0 < x < 2\pi(N-1)/\ell$ for some ℓ, its depth profile being of the form

$$h(x) = h_0 - d\,(\sin(\ell x) + \sin(m\ell x))\,, \tag{5.5}$$

which is sufficiently general for our purposes.

Note that, when using the approximate mild-slope equation, the approximate modified mild-slope equation or Kirby's extended mild-slope equation, it is the term $d(\sin(\ell x) + \sin(m\ell x))$ which plays the role of δ referred to in Section 4.

In the first example we consider, we take $m = 0$ and $d/h_0 = 0.16$. The topography therefore consists of a patch of $N - 1$ sinusoidal ripples. We shall ultimately examine the scattering characteristics of waves over 10 such ripples by taking $N = 11$. However the replication formulae and resonance analysis allow us to consider the one ripple (i.e. $N = 2$) case and make predictions about larger N from the simpler case.

Figure 1 shows graphs of $|R_{1,2}|$ plotted against $2k/\ell$ for the mild-slope equation, the modified mild-slope equation and Kirby's extended mild-slope equation. The corresponding curves for the approximate mild-slope equation and the approximate modified mild-slope equation are very much like their unapproximated counterparts and are omitted from the graph for clarity. That the three curves shown are markedly different, but it is significant that the modified mild-slope equation and the extended mild-slope equation give approximations which are very close to each other near $2k/\ell = 1$.

Figure 2 shows γ, defined in (5.2), also plotted against $2k/\ell$ for the modified mild-slope equation. The γ curves for all five models referred to in Section 4 are so similar as to be virtually indistinguishable on the scale used in the figure. As our ultimate interest is to examine how resonance occurs for 10 ripples the lines $\cos(\alpha\pi/10)$, $\alpha = 1, 2, \ldots, 9$ are also shown on Figure 2. We recall from Section 3 that the intersections of these lines with the γ curve coincide with the positions of the zeros of $|R_{1,11}|$.

Resonance will occur in those intervals where $|\gamma| > 1$, but these cannot be identified clearly from Figure 2. However, since $|\gamma| > 1$ if and only if $\mathrm{Im}(\theta) = \mathrm{Im}(\cos^{-1}\gamma) \neq 0$, we can determine the resonance bands by plotting $\mathrm{Im}(\theta)$. This is done in Figure 3 for the mild-slope equation and modified mild-slope equation. The corresponding graph for the approximate mild-slope equation is virtually indistinguishable from Figure 3(i) and the graph for the approximate modified mild-slope equation is almost exactly like Figure 3(ii), except that the peak near $2k/\ell = 2$ is missing. The graph of $\mathrm{Im}(\theta)$ for the extended mild-slope equation is also very like Figure 3(ii), but again without the second peak. It is clear from these figures that only the modified mild-slope equation will detect resonance near $2k/\ell = 2$ and that the mild-slope equation will produce smaller resonances near $2k/\ell = 1$ since we already know from Figure 1 that its approximation to $|R_{1,2}|$ is smaller there than

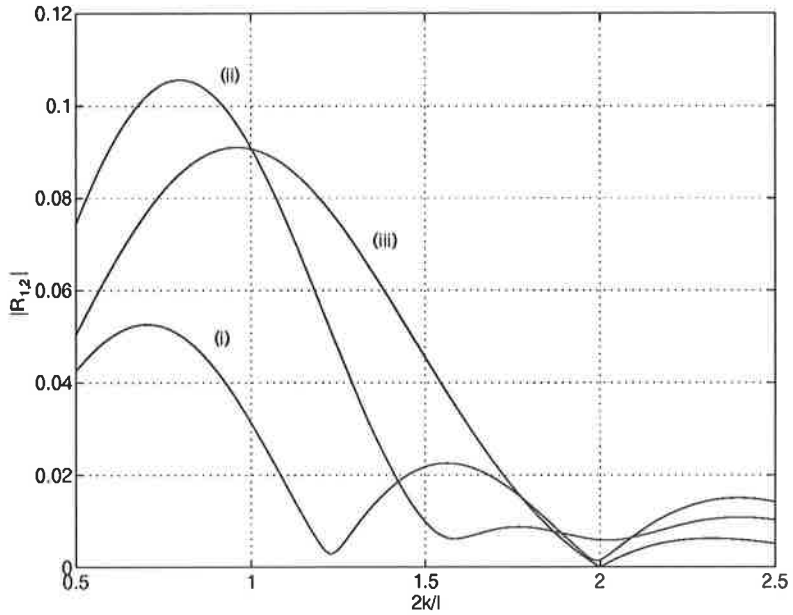

Figure 1: $|R_{1,2}|$ for the mild-slope equation (i), the modified mild-slope equation (ii) and Kirby's extended mild-slope equation (iii) for one sinusoidal ripple with $d/h_0 = 0.16$.

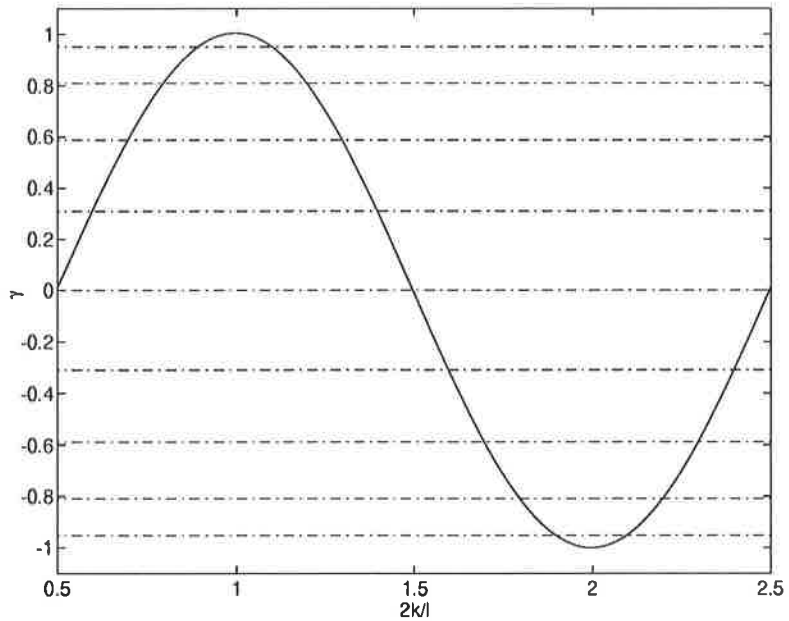

Figure 2: Graph of γ using the modified-mild slope equation for one sinusoidal ripple with $d/h_0 = 0.16$. The positions of the zeros of $|R|$ for the 10 ripple case are indicated using broken lines

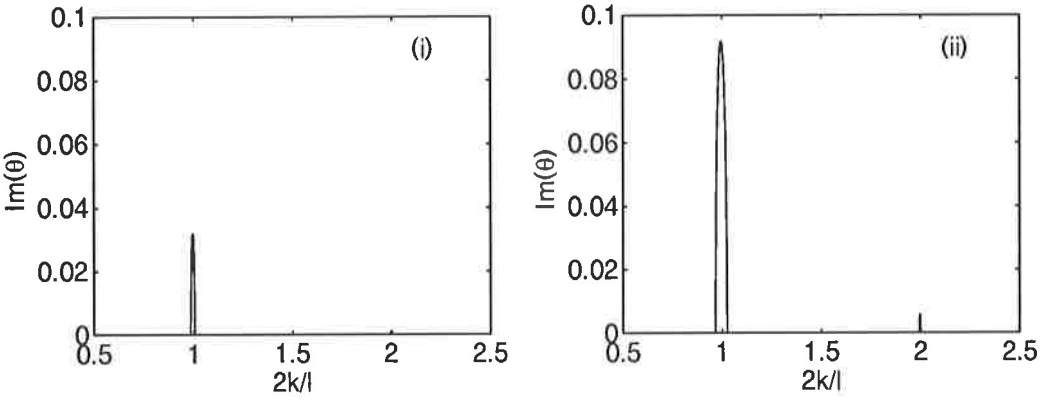

Figure 3: $\mathrm{Im}(\theta)$ using the mild-slope equation (i) and the modified mild-slope equation (ii) for one sinusoidal ripple with $d/h_0 = 0.16$.

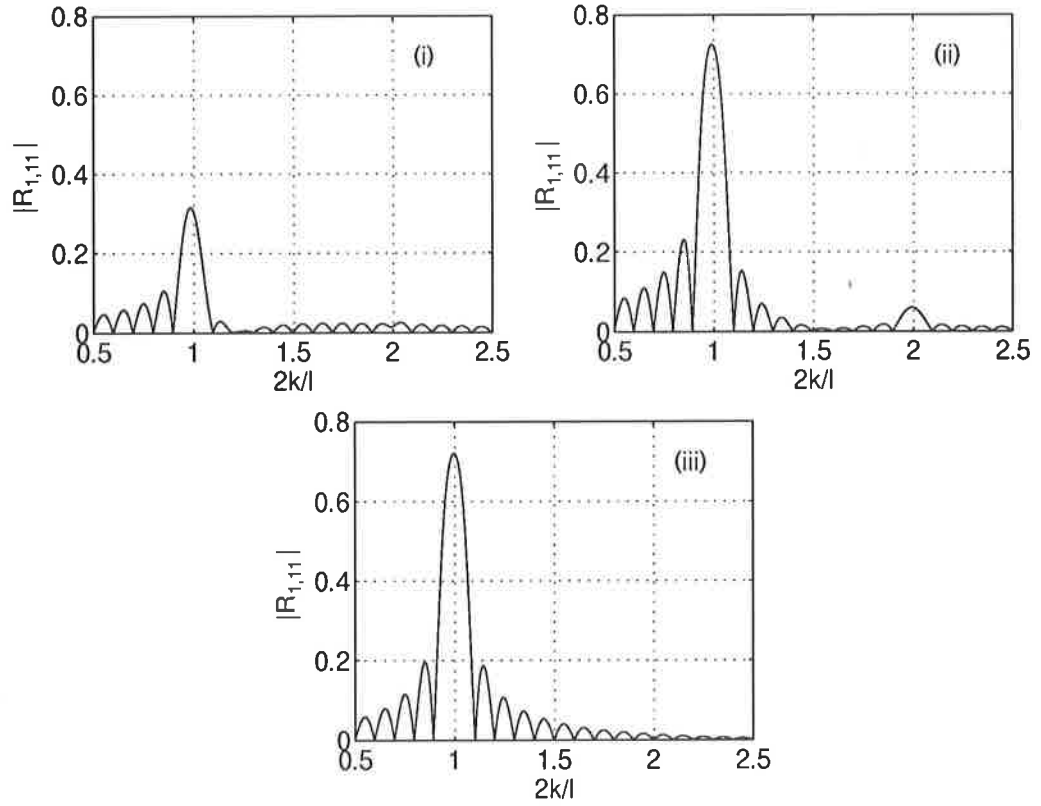

Figure 4: Comparison of reflected amplitudes for a patch of 10 sinusoidal ripples with $d/h_0 = 0.16$ using the mild-slope equation (i), the modified mild-slope equation (ii) and the extended mild-slope equation (iii)

that given by using the modified mild-slope equation.

One prediction we can make at this point concerns the size of the resonant peak near $2k/\ell = 1$ for the modified mild-slope equation and the extended mild-slope equation. It has been observed that the graphs of $\mathrm{Im}(\theta)$ for these two models are almost identical and we have seen that values of $|R_{1,2}|$ are very similar near $2k/\ell = 1$. These two facts are sufficient to tell us that, despite the other differences in the two models evident in Figure 1, the resonant peaks for these two models will be largely identical as N increases.

Figure 4 serves to verify the predictions made above. Graphs of $|R_{1,11}|$ are shown for the mild-slope equation, the modified mild-slope equation and Kirby's mild-slope equation. The figure confirms that

1 The zeros of $|R_{1,11}|$ occur where γ cuts the lines $\cos(\alpha\pi/10)$, $\alpha = 1, 2, \ldots, 9$ and are virtually identical for all of the model equations;

2 Only the modified-mild slope equation shows any resonant behaviour near $2k/\ell = 2$;

3 The principal resonances obtained using the modified mild-slope equation and the extended mild-slope equation are very similar despite the differences in $|R_{1,2}|$ for these models.

In the second example we take $m = 1.5$ and $d/h_0 = 0.33$ in (5.5). In this case the bed form does not have period $2\pi/\ell$ but rather $4\pi/\ell$. Our ultimate aim here is to consider the case where $N = 9$, corresponding to 8 sinusoidal ripples superimposed on 12 sinusoidal ripples. In order to use our replication formulae we must divide the ripple patch into 4 regions each of length $4\pi/\ell$. Thus, in the notation of Section 2, we set $l_j = 4\pi(j-1)/\ell$ $j = 1, 2, \ldots, 5$, and we take $N = 5$ to obtain the effects of the full bed.

Figure 5 shows graphs of $|R_{1,2}|$ plotted against $2k/\ell$ for the mild-slope equation, the modified mild-slope equation and Kirby's extended mild-slope equation. The corresponding curves for the approximate mild-slope equation and the approximate modified mild-slope equation are very much like their unapproximated counterparts and are again omitted from the graph.

In Figure 6 the γ curve corresponding to the modified mild-slope equation is shown; the corresponding γ curves for the other four models are the same, as far as the eye can distinguish. The broken lines are at $\cos(\alpha\pi/4)$, $\alpha = 1, 2, 3$ and cut the γ curve at the zeros of $|R_{1,5}|$.

In Figure 7 we give graphs of $\mathrm{Im}(\theta)$ for the mild-slope equation and modified mild-slope equation showing the intervals in which resonance will occur. The heights of the peaks of $\mathrm{Im}(\theta)$ taken in conjunction with the value of $|R_{1,2}|$

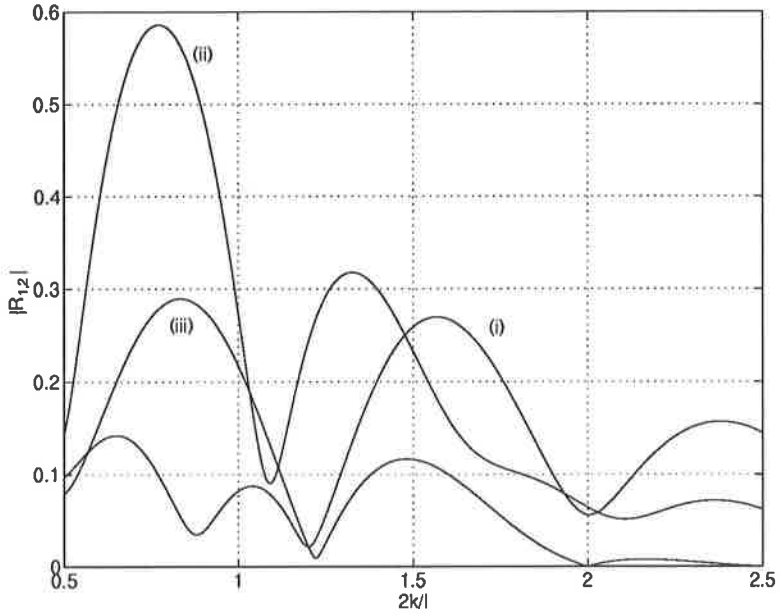

Figure 5: $|R_{1,2}|$ for the mild-slope equation (i), the modified mild-slope equation (ii) and Kirby's extended mild-slope equation (iii) for one period of the doubly-sinusoidal ripple with $d/h_0 = 0.33$.

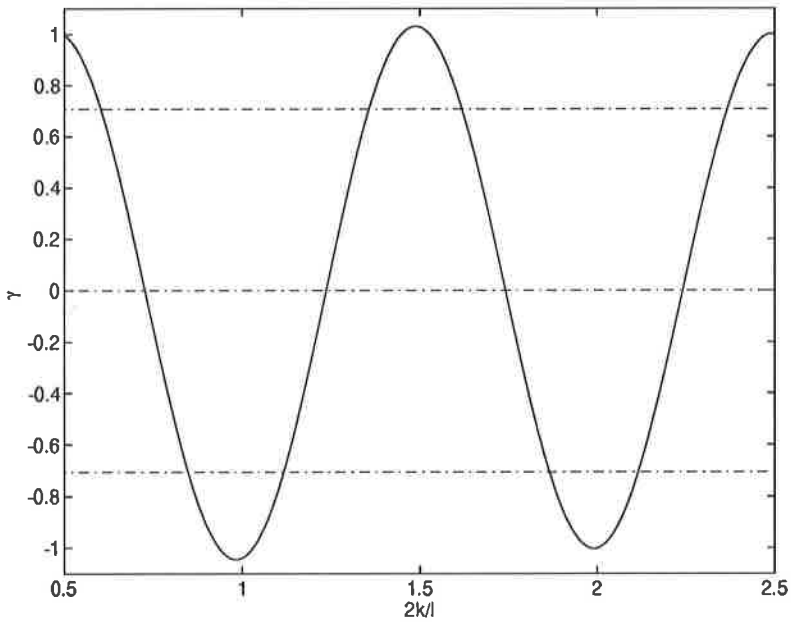

Figure 6: Graph of γ using the modified-mild slope equation for one period of the doubly-sinusoidal ripple with $d/h_0 = 0.33$. The positions of the zeros of $|R|$ for the $N = 4$ case are indicated using broken lines

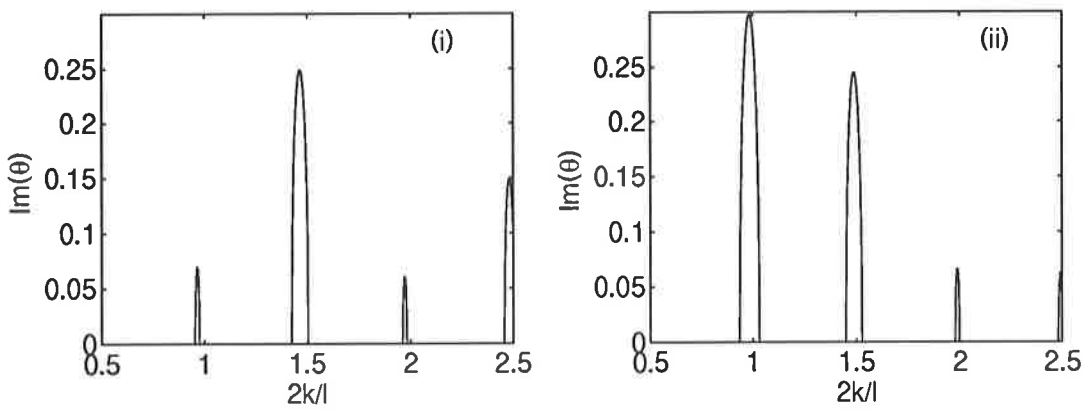

Figure 7: Im(θ) using the mild-slope equation (i) and the modified mild-slope equation (ii) for one period of the doubly-sinusoidal ripple with $d/h_0 = 0.33$.

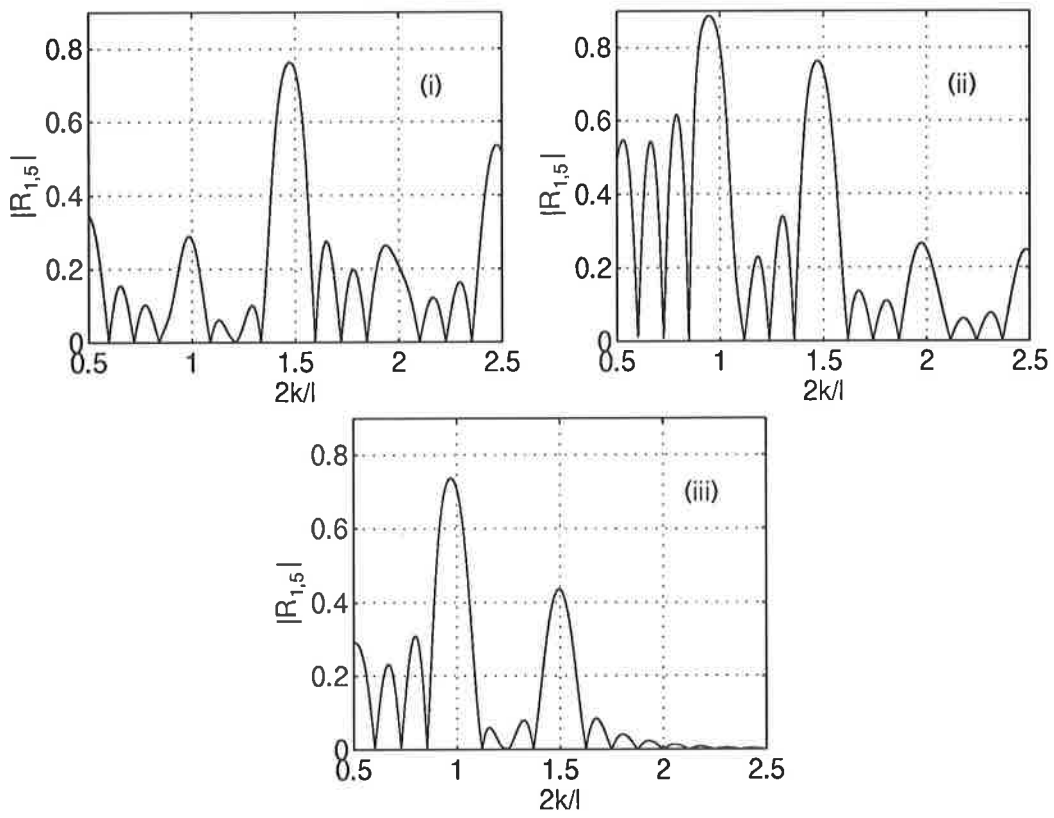

Figure 8: Comparison of reflected amplitudes for a patch of 8 sinusoidal ripples onto which 12 sinusoidal ripples are superimposed where $d/h_0 = 0.16$. Approximations used are the mild-slope equation (i), the modified mild-slope equation (ii) and the extended mild-slope equation (iii)

at that value of $2k/\ell$ indicate the heights of the resonant peaks. This feature is confirmed in Figure 8 where graphs of $|R_{1,5}|$ are shown for the mild-slope equation and the modified mild-slope equation. The corresponding graph for the extended mild-slope equation is included for comparison.

References

[1] Berkhoff, J. C. W., "Computation of combined refraction-diffraction", *Proc. 13th Int. Conf. on Coastal Eng., July 1972, Vancouver, Canada. ASCE, New York, N. Y. (1973), 471-490,* (1972).

[2] Berkhoff, J. C. W., "Mathematical models for simple harmonic linear water waves", *Delft Hydr. Rep. W 154-IV,* (1976).

[3] Chamberlain, P. G., "Wave scattering over uneven depth using the mild-slope equation", *Wave Motion, 17,* 267-285 (1993).

[4] Chamberlain, P. G., "Symmetry relations and decomposition for the mild-slope equation", *J. Eng. Math. (to appear).*

[5] Chamberlain, P. G., & Porter, D., "The modified mild-slope equation", *Submitted.*

[6] Ince, E. L., *Ordinary Differential Equations,* Dover (1944).

[7] Kirby, J. T., "A general wave equation for waves over rippled beds", *J. Fluid Mech., 162,* 171-186 (1986).

[8] Lambert, J. D., *Numerical Methods for Ordinary Differential Systems,* Wiley (1992).

[9] Newman, J. N., "Propagation of water waves past long two-dimensional obstacles", *J. Fluid Mech., 23,* 23-29 (1965).

Appendix

The objective is to solve (3.5) for the components of $S_{1,N}$ on the assumptions that $T_{1,2} \neq 0$ and $T_{1,2} = T_{2,1}$. The relationship

$$1 - R_{1,2}R_{2,1} + T_{1,2}^2 = 2\gamma T_{1,2}, \qquad \gamma = \frac{\cos(\arg(T_{1,2}))}{|T_{1,2}|}, \tag{A1}$$

which follows from (2.11), simplifies the algebra.

We first determine Δ_n, noting from (3.5c), (3.6) and (A1) that

$$\begin{aligned} \Delta_{n+1} &= 2\gamma T_{1,2} - \Delta_n^{-1} T_{1,2}^2 \qquad (n = 2, 3, \ldots, N-1), \\ \Delta_2 &= 2\gamma T_{1,2} - T_{1,2}^2. \end{aligned}$$

If we put $\Delta_n = T_{1,2} u_n / u_{n-1}$ $(n = 2, 3, \ldots, N)$ and define $u_1 = 1$, we easily find that $u_2 = 2\gamma - T_{2,1}$ and that

$$u_{n+1} - 2\gamma u_n + u_{n-1} = 0 \qquad (n = 2, 3, \ldots, N-1),$$

which allows $u_3, u_4, \ldots, u_N$, and therefore $\Delta_3, \Delta_4, \ldots, \Delta_N$, to be calculated.

In fact, since $R_{1,2} R_{N,1} = 1 - \Delta_N$, by (3.6), we at once have

$$R_{1,2} R_{N,1} = \frac{u_{N-1} - T_{1,2} u_N}{u_{N-1}}. \tag{A2}$$

Also (3.5b) can be written in the form $T_{1,n+1} = T_{1,n} u_{n-1} / u_n$, repeated use of which gives

$$T_{1,N} = \frac{T_{1,2}}{u_{N-1}}. \tag{A3}$$

By using (3.5a) and (3.5d), or (2.11), it can now be shown that

$$R_{2,1} R_{1,N} = R_{1,2} R_{N,1}, \qquad T_{N,1} = T_{1,N}. \tag{A4}$$

Formulae which are practically more convenient are obtained on replacing the sequence (u_n) of complex numbers by a new sequence (σ_n) of real numbers. This is achieved by setting $R_{1,2} R_{2,1} \sigma_n = u_{n-1} - T_{1,2} u_n$, which implies that $u_n = \sigma_{n+1} - T_{1,2} \sigma_n$ and that $\sigma_{n+1} - 2\gamma\sigma_n + \sigma_{n-1} = 0$ $(n = 2, 3, \ldots, N-1)$, together with $\sigma_1 = 0$ and $\sigma_2 = 1$. The formulae (A2) and (A3) imply that

$$R_{1,N} = \frac{R_{1,2} \sigma_N}{\sigma_N - T_{1,2} \sigma_{N-1}}, \qquad T_{1,N} = \frac{T_{1,2}}{\sigma_N - T_{1,2} \sigma_{N-1}},$$

(A4) remaining unchanged.

Finally, it is easy to show that $\sigma_n^2 - \sigma_{n-1} \sigma_{n+1} = 1$ $(n = 2, 3, \ldots, N-1)$ and hence that $|\sigma_N - T_{1,2} \sigma_{N-1}|^2 = |R_{1,2}|^2 \sigma_N^2 + |T_{1,2}|^2$.

A summary of the formulae obtained here is given in the main body of the text.